

## Time-delayed entanglement from coherently coupled nonlinear cavities

Terry G. McRae<sup>1,2</sup> and Warwick P. Bowen<sup>1</sup>

<sup>1</sup>*School of Mathematics and Physics, University of Queensland, Brisbane, Queensland 4072, Australia*

<sup>2</sup>*Department of Physics, MacDiarmid Institute, University of Otago, Dunedin 9054, New Zealand*

(Received 19 January 2009; revised manuscript received 8 June 2009; published 9 July 2009)

The output fields of a pair of coherently coupled nonlinear optical cavities are found to exhibit strong optical entanglement. For sufficiently strong coupling time-delayed quantum correlations are observed providing a resource for quantum information protocols such as all-optical quantum memories. A straightforward experimental implementation applicable to whispering gallery mode resonators such as microtoroids is proposed.

DOI: [10.1103/PhysRevA.80.010303](https://doi.org/10.1103/PhysRevA.80.010303)

PACS number(s): 03.67.Bg, 03.67.Hk, 42.50.Pq, 42.65.Lm

### I. INTRODUCTION

In the last century, interest in entanglement was motivated predominately by its fundamental significance as “the characteristic trait of quantum mechanics” [1]. In recent years, however, a paradigm shift has occurred due to the realization that entanglement can facilitate powerful measurement, computation, and communication tasks [2]. Optical entanglement is of particular significance, both enabling applications such as quantum cryptography, quantum information networks, and quantum metrology [2] and facilitating the most stringent tests of quantum mechanics performed to date [3].

Here we investigate optical entanglement generated from a pair of coherently coupled nonlinear optical cavities. Coherently coupled optical cavities are of fundamental interest enabling for example an all-optical analog to electromagnetically induced transparency (EIT) [4] with the capacity to both slow and stop light [5]. Consistent with previous work on nonlinear coupled intracavity waveguides [6], we show that the introduction of nonlinearity enables arbitrarily strong entanglement to be generated. Interestingly, however, for strong coupling, the entanglement is quenched and a new form of entanglement exhibiting time-delayed quantum correlations becomes apparent. This entanglement is analogous to that generated in  $\lambda$ -type atomic ensemble quantum memories [7], which have already proved to be an enabling technology in quantum information applications such as quantum repeaters and on-demand single photon sources [8]. In contrast to atomic ensembles, quantum memory capabilities are not typically available in nonlinear optical systems. Indeed, they are only present in our system due to the EIT-like nature of the coupled cavities and to our knowledge have not been predicted for any other nonlinear optics based entanglement source. The time-delayed entanglement predicted here has many applications in quantum information science. For example, an all-optical quantum memory could be implemented utilizing time-delayed entanglement as the nonclassical resource for quantum teleportation [9].

This Rapid Communication models a pair of identical below threshold coherently coupled optical parametric oscillators (OPOs) each consisting of a  $\chi^{(k+1)}$  general nonlinear medium enclosed in an optical cavity as shown in Fig. 1(a). Such a configuration is experimentally relevant, most notably to ultrahigh quality whispering gallery mode (WGM) resonators where counterpropagating modes are coupled by scattering centers [10] as shown in Fig. 1(b). Silica microtoroidal resonators [10] and polished crystal microdisks [11],

for example, respectively exhibit high  $\chi^{(3)}$  and  $\chi^{(2)}$  nonlinearity, as well as strong scattering. These resonators are capable of providing strong optical confinement in a scalable, robust, microfabricated architecture with high coupling efficiency to optical fiber [10]. They are therefore an ideal candidate to produce, in-fiber, the strong entanglement predicted here. Such entanglement would be an important resource for scalable quantum information networks, as well as long-distance fundamental tests of quantum mechanics such as the EPR paradox [12] and Bell tests [3]. Furthermore, recent research has demonstrated an exquisite capability to engineer microresonator mechanical properties [13] providing the potential to suppress noise due to guided wave Brillouin and Raman scattering, which presents a strong constraint on existing in-fiber entanglement sources [14].

### II. ANALYSIS

Our model is closely analogous to that used previously to analyze nonclassical states from a pair of coupled intracavity nonlinear waveguides [6]. Within each coupled OPO cavity the nonlinear process converts  $k$  pump photons at frequency  $\omega_p$  into a pair of signal and idler photons at frequencies  $\omega_1 = \Omega - \Delta'$  and  $\omega_2 = \Omega + \Delta'$ , where to maintain energy conservation  $\Omega = \frac{k}{2}\omega_p$ . Since the pump fields in such systems are typically bright we treat them classically here, with  $\alpha_x$  and  $\alpha_y$  denoting their coherent amplitudes, and the subscripts  $x$  and  $y$  used throughout to distinguish the two cavity modes. Assuming the nonlinear interaction strength  $\Gamma$  is identical for modes  $x$  and  $y$ , and the coherent coupling rate  $g$  is independent of detuning  $\Delta'$ , as is the experimentally relevant case, and taking the rotating wave approximation yields the system Hamiltonian [6]

$$H^{(k+1)} = \hbar \sum_{n=1}^2 \left[ g(\hat{a}_{xn}\hat{a}_{yn}^\dagger + \hat{a}_{xn}^\dagger\hat{a}_{yn}) + \sum_m \omega_{mn}\hat{a}_{mn}^\dagger\hat{a}_{mn} \right] + i\hbar\Gamma \sum_m (\alpha_m^k \hat{a}_{m1}^\dagger \hat{a}_{m2}^\dagger - \alpha_m^{k*} \hat{a}_{m1} \hat{a}_{m2}), \quad (1)$$

where  $m \in \{x, y\}$ ,  $\hat{a}$  is the annihilation operator, and the subscripts 1 and 2 denote the signal and idler fields respectively. Assuming both cavity modes  $x$  and  $y$  have identical input coupling and loss rates, denoted by  $\gamma_{in}$  and  $\gamma_l$ , respectively, as is typical for experimental systems, and applying the quantum Langevin equation [15] to Eq. (1) we obtain four

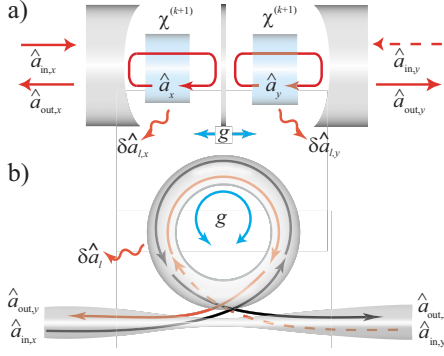


FIG. 1. (Color online) Schematics of coupled cavity systems. (a) Two optical cavities coupled via a partially reflective mirror, each containing a  $(k+1)$ th order nonlinear medium. (b) An equivalent WGM resonator with two counterpropagating optical modes coupled by optical scattering and intrinsic nonlinearity.

equations of motion for the signal and idler fields,

$$\dot{\hat{a}}_{x1} = \Gamma \alpha_x^k \hat{a}_{x2}^\dagger - (\gamma + i\Delta') \hat{a}_{x1} - ig' \hat{a}_{y1} - \sqrt{2\gamma_{in}} \hat{a}_{in,x1} + \sqrt{2\gamma_l} \hat{a}_{l,x1},$$

$$\dot{\hat{a}}_{x2} = \Gamma \alpha_x^k \hat{a}_{x1}^\dagger - (\gamma - i\Delta') \hat{a}_{x2} - ig' \hat{a}_{y2} - \sqrt{2\gamma_{in}} \hat{a}_{in,x2} + \sqrt{2\gamma_l} \hat{a}_{l,x2},$$

$$\dot{\hat{a}}_{y1} = \Gamma \alpha_y^k \hat{a}_{y2}^\dagger - (\gamma + i\Delta') \hat{a}_{y1} - ig' \hat{a}_{x1} - \sqrt{2\gamma_{in}} \hat{a}_{in,y1} + \sqrt{2\gamma_l} \hat{a}_{l,y1},$$

$$\dot{\hat{a}}_{y2} = \Gamma \alpha_y^k \hat{a}_{y1}^\dagger - (\gamma - i\Delta') \hat{a}_{y2} - ig' \hat{a}_{x2} - \sqrt{2\gamma_{in}} \hat{a}_{in,y2} + \sqrt{2\gamma_l} \hat{a}_{l,y2},$$

where  $\hat{a}_{in}$  and  $\hat{a}_l$  are the fields entering through the input coupler and loss mechanisms, respectively, and  $\gamma = \gamma_{in} + \gamma_l$  is the total decay rate of each cavity. Assuming  $\alpha_x$  and  $\alpha_y$  are independent of time these equations can be solved in the frequency domain by taking the Fourier transform. The dimensionless quantities  $R_x = \frac{\Gamma |\alpha_x|^k}{\gamma}$ ,  $R_y = \frac{\Gamma |\alpha_y|^k}{\gamma}$ ,  $g = g'/\gamma$ ,  $\Delta = \Delta'/\gamma$ , and  $\eta = \gamma_{in}/\gamma$  are used, where  $\eta$  is the cavity escape efficiency and  $R$  is a dimensionless pump strength with the physical significance that  $R=1$  corresponds to the OPO threshold. The solution can then be expressed compactly as  $\frac{1}{2} \hat{M} \hat{A} = \sqrt{\eta} \hat{A}_{in} + \sqrt{1-\eta} \hat{A}_l$ , where

$$\hat{M} = \begin{bmatrix} i\Delta - 1 & R_x e^{ik\phi_x} & -ig & 0 \\ R_x e^{ik\phi_x} & i\Delta - 1 & 0 & ig \\ -ig & 0 & i\Delta - 1 & R_y e^{ik\phi_y} \\ 0 & ig & R_y e^{-ik\phi_y} & i\Delta - 1 \end{bmatrix}, \quad (2)$$

$\phi_x$  and  $\phi_y$  are the phases of the two pumps, and throughout vectors  $\hat{A}_q$  are of the form  $\hat{A}_q = [\hat{a}_{q,x1}, \hat{a}_{q,x2}^\dagger, \hat{a}_{q,y1}, \hat{a}_{q,y2}^\dagger]^T$ .

One can then use the input/output relations  $\hat{A}_{out} = \sqrt{2\gamma_{in}} \hat{A} + \hat{A}_{in}$  [15] to solve for the output fields,

$$\hat{A}_{out} = [I_4 + 2\eta \hat{M}^{-1}] \hat{A}_{in} + 2\sqrt{\eta(1-\eta)} \hat{M}^{-1} \hat{A}_l, \quad (3)$$

where  $I_4$  is the  $4 \times 4$  identity matrix. General output field quadratures for each of the four system modes are then readily obtained as  $\hat{X}^\theta(\Delta) = \hat{a}(\Delta) e^{-i\theta} + \hat{a}^\dagger(\Delta) e^{i\theta}$ .

Any entanglement generated by our coupled cavity system is expected to display Gaussian statistics since the fluctuations of all input fields are Gaussian and the nonlinear

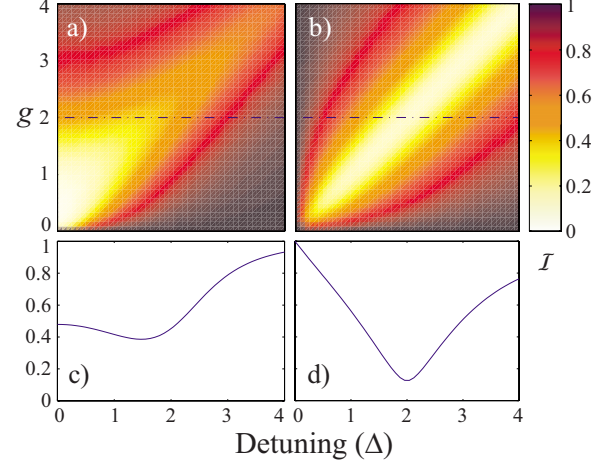


FIG. 2. (Color online) Inseparability as a function of detuning  $\Delta$  and coupling rate  $g$ . (a) and (c) Undelayed entanglement with  $\Delta\phi = \phi_x - \phi_y = 0$ ; (b) and (d) time-delayed entanglement with  $\Delta\phi = \pi/k$ . Model parameters:  $R_x = R_y = 0.9$  and  $\eta = 0.99$ .

processes involved retain this Gaussian character. Gaussian continuous variable entanglement between orthogonal field quadratures pairs of two light beams can be completely characterized by the correlation matrix of the system, which can be constructed in our case from Eq. (3) for any two pairs of output fields. Here we follow the procedure of Duan *et al.* [16] for bipartite continuous variable systems, who showed that the correlation matrix of any Gaussian state can be transformed reversibly into a standard form, from which the *degree of inseparability*  $\mathcal{I}$  can be defined such that  $\mathcal{I} < 1$  is a necessary and sufficient condition for two-mode entanglement, with maximal entanglement characterized by  $\mathcal{I} = 0$ . The degree of inseparability is the standard tool for experimental characterizations of continuous variable entanglement due to ease of both measurement and interpretation [7, 17, 18]. We use the method of Grosse *et al.* [17] to numerically calculate the degree of inseparability from the output field correlation matrix of the coupled cavity system.

### III. RESULTS

In general, entanglement can be observed between the fields  $\hat{a}_{x1}$ ,  $\hat{a}_{x2}$ ,  $\hat{a}_{y1}$ , and  $\hat{a}_{y2}$  through direct individual measurements on each. However, here we consider the more experimentally realistic situation of heterodyne detection performed separately on the outputs of each of the subsystems  $x$  and  $y$  with a local oscillator at frequency  $\Omega$ . In this case for each subsystem both signal and idler fields  $\hat{a}_{m1}$  and  $\hat{a}_{m2}$  beat with the local oscillator and, combined, produce a signal directly proportional to the joint-quadrature operator

$$\tilde{X}_{m,t}^\theta(\Delta) = \frac{1}{\sqrt{2}} [\hat{X}_{m,1}^{\Delta',t+\theta}(\Delta) + \hat{X}_{m,2}^{-\Delta',t+\theta}(\Delta)], \quad (4)$$

where  $m \in \{x, y\}$ ,  $\theta$  is the local oscillator phase, and  $t$  is the time at which the measurement occurs. As a result of the frequency difference between the signal and idler fields we see that a time delay has the effect of rotating the observed

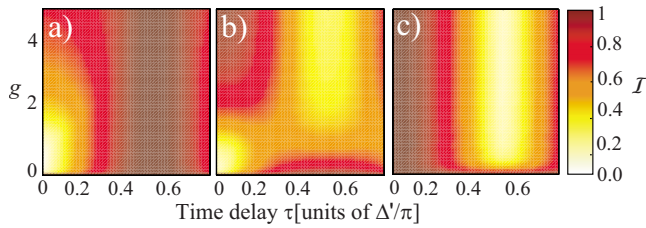


FIG. 3. (Color online) Inseparability as a function of measurement time delay optimized over detuning. (a)  $\Delta\phi=0$ , (b)  $\Delta\phi=\pi/2k$ , and (c)  $\Delta\phi=\pi/k$ . Model parameters:  $R_x=R_y=0.9$  and  $\eta=0.99$ .

signal and idler quadratures in opposite directions. Entanglement of the orthogonal quadrature pair  $\tilde{X}_{x,\tau_x}^{\theta_x}(\Delta)$  and  $\tilde{X}_{x,\tau_x}^{\theta_x+\pi/2}(\Delta)$  of field  $x$  with the equivalent quadratures of field  $y$  is possible due to the Heisenberg uncertainty relation  $\Delta^2 X_m^\theta \Delta^2 X_m^{\theta+\pi/2} \geq 1$ , which originates from the commutation relation  $[\tilde{X}_m^\theta, \tilde{X}_m^{\theta+\pi/2}] = 2i$ . We analyze entanglement of this kind henceforth and restrict our analysis to the optimal situation where  $\theta_x = \theta_y = \theta$ .

In all nonlinear optics based entanglement sources to date, due to the near instantaneous response of the nonlinearity, the quantum correlations between output fields are observed without time delay. Hence, here we begin by considering the case where the output fields are measured at the same time, i.e.,  $t_x = t_y$ . Figures 2(a) and 2(c) illustrate the degree of inseparability calculated for this case as a function of coupling rate and detuning from cavity resonance, where we have chosen equal intensity in-phase pump fields and parameters typically achieved in experiments. Strong entanglement is observed. When  $g \ll 1$  the best entanglement is near resonance as one might perhaps expect. However for large coupling one observes both that the entanglement is quenched and that the maximum entanglement shifts to nonzero detuning. The shift can be understood from the well-known mode splitting that occurs in coupled cavity systems [6,10]. As a result fields produced at frequencies detuned by  $g$  from the unperturbed resonance frequencies are on resonance within the cavity and the nonlinear response is enhanced. The entanglement quenching, however, is surprising since the coupling is a reversible process. To investigate this further we consider the

time-delayed case where the measurement on field  $x$  is delayed by a time  $\tau = t_x - t_y$ .

Figure 3 shows the evolution of entanglement with measurement time delay for three different relative pump phases  $\Delta\phi = \phi_x - \phi_y$ , where we have optimized the inseparability over detuning  $\Delta$  as is typically performed in experiments using spectral analysis. In Fig. 3(a) the pumps are in phase and we see the normal behavior for a nonlinear optics based entanglement source, with maximal entanglement when there is no time delay ( $\tau=0$ ), and as seen before in Figs. 2(a) and 2(c) a strong dependence on  $g$ , with entanglement optimized at  $g \approx 0.5$ . In Fig. 3(b) a pump phase delay of  $\pi/2k$  is introduced and we see an overall reduction in the level of entanglement. However, now as the coupling rate increases and the undelayed entanglement is quenched, a transition occurs to time-delayed entanglement, with a delay between detection events of  $\tau = \pi/2\Delta'$ . In contrast, this time-delayed entanglement is optimized at large  $g$ . In Fig. 3(c) where  $\Delta\phi = \pi/k$  the undelayed entanglement is no longer apparent for any  $g$ , with time-delayed entanglement present for all but very small  $g$ . The dependence of the degree of inseparability on coupling rate and detuning for this time-delayed case are shown in Figs. 2(b) and 2(d). It is clear that now the maximum entanglement always occurs at  $\Delta = g$ , can be shifted far from the resonance frequency of the cavity, and is insensitive to  $g$  for  $g \gg 1$ . This resonance frequency shift is technically significant, allowing the optimal entanglement to be moved away from low frequency noise sources such as the laser relaxation oscillation which typically limit both entanglement strength and purity.

A standard method of generating optical entanglement is to interfere a pair of squeezed beams on a 50/50 beam splitter [18], with the relative phase being critical to the strength of the entanglement. In an analogous manner the coherent coupling in our scheme interferes the nonclassical fields generated in the two cavity modes. In contrast, however, here the coherent coupling also affects the relative phase of the interference. It is this phase effect which is ultimately responsible for both the change in relative pump phase required to achieve strong entanglement when  $g \gg 1$  and the time-delayed correlations exhibited by such entanglement. The mechanism is through rotation of the quantum correlated field quadratures. The signal and idler fields output from

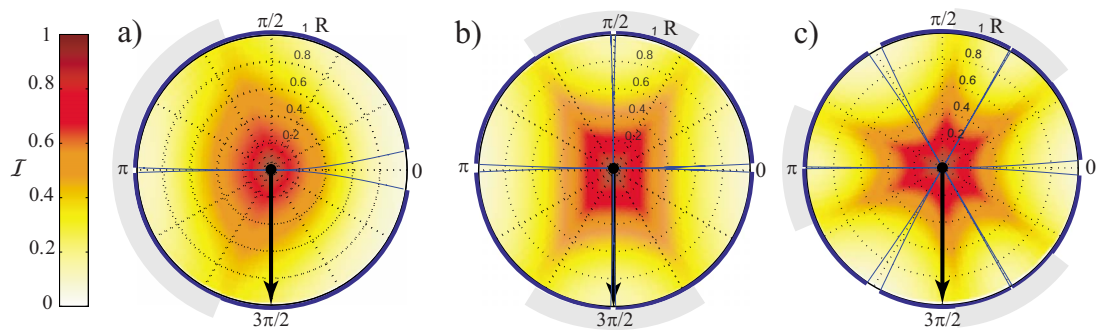


FIG. 4. (Color online) Dependence of inseparability on pump strength  $R=R_x=R_y$  (radial axis) and relative phase  $\Delta\phi$  (azimuthal axis), optimized over  $\Delta$  and  $\tau$ . Order of nonlinearity: (a)  $\chi^{(2)}$  ( $k=1$ ), (b)  $\chi^{(3)}$  ( $k=2$ ), and (c)  $\chi^{(4)}$  ( $k=3$ ). Dark lines circumscribe sectors of 4-partite entanglement; gray bands circumscribe sectors dominated by time-delayed entanglement. Arrow: path followed for single sided pumping. Model parameters:  $\eta=0.99$  and  $g=1$ . The plot sectors are effectively compressed by  $\pi/k$  as the order of the nonlinearity increases.

mode  $x$ , respectively, experience  $\pi/2$  and  $-\pi/2$  phase rotations compared to their counterparts from mode  $y$ . Although a pump path length change smaller than the optical wavelength is sufficient to cause this rotation, rephasing to allow observation of the resulting time-delayed entanglement requires a path length increase of  $c\tau = \pi c/2\Delta$  on output field  $x$ , which for a typical experimental detuning of 1 MHz corresponds to a far longer length of 75 m. Thus the phase effect due to coherent coupling has, through the nonlinear process, been transformed to a substantial delay in the quantum correlations between the fields. Since this is inherently a phase effect between the signal and idler modes, it is worth noting that identical results could be achieved by delaying output field  $y$  (rather than  $x$ ).

Figure 4 compares how the relative pump phase  $\Delta\phi$  affects the entanglement achievable in our system for  $\chi^{(2)}$ ,  $\chi^{(3)}$ , and  $\chi^{(4)}$  nonlinearities. The minimum degree of inseparability between the output fields optimized over time delay and detuning is calculated as a function of relative pump phase and pump strength. The optimal time delay is found always to be either  $\tau=0$  or  $\pi/2\Delta'$ . We see that for all orders of nonlinearity the entanglement increases with increasing pump strength. As expected, there is a strong dependence on  $\Delta\phi$ . However for high pump strength substantial entanglement can be generated for all  $\Delta\phi$  in distinct contrast to conventional entanglement sources such as the squeezed beam interferometers discussed above where entanglement generation fails in some regions. A coupling rate of  $g=1$  is chosen for the results in Fig. 4 allowing both undelayed and delayed entanglement to exist simultaneously [see Fig. 3(b)]. Where this occurs, the system exhibits time-delayed 4-partite entanglement, where the time-delayed and non-time-delayed outputs of  $x$  are both entangled to both time-delayed and non-time-delayed outputs of  $y$ . The sectors of Fig. 4 circumscribed by the dark line indicate the parameter regimes where 4-partite entanglement exists. We see that such entanglement is apparent throughout the majority of the parameter space. This multipartite entanglement will be investigated further in future work.

Finally we turn our attention to a robust and straightforward experimental implementation of bipartite entanglement. Consider the case where only cavity mode  $x$  is directly pumped with mode  $y$  pumped indirectly through coherent coupling from mode  $x$ . In this case one finds that  $\alpha_y = ig\alpha_x$ . Hence the relative phase between the pumps is  $\Delta\phi = 3\pi/2$ , so that when  $g=1$  single sided pumping tracks the downward facing arrow in Fig. 4. We see that in the special case of  $\chi^{(3)}$  nonlinearity relevant to silica microtoroidal resonators [10] optimum entanglement can be achieved naturally in this single sided pumping scenario. For this case the simple analytical solution

$$\mathcal{I} = \sqrt{1 - \frac{16\eta R[\Delta - R(1 - \eta)]}{[(1 + R)^2 + (\Delta - 1)^2][(1 - R)^2 + (\Delta + 1)^2]}}, \quad (5)$$

for the inseparability can be obtained. It is clear that as  $\{R, \eta, \Delta\} \rightarrow 1$ ,  $\mathcal{I} \rightarrow 0$ . Hence for sufficiently strong pumping and high efficiency, strong entanglement can be generated with only a single external pump field.

In conclusion, we have shown that strong entanglement can be generated between the output fields of a pair of coherently coupled nonlinear optical cavities. For sufficiently strong coupling, the quantum correlations become time delayed and can therefore be used in conjunction with quantum teleportation to achieve an all-optical quantum memory. A straightforward experimental implementation applicable to ultrahigh quality WGM microresonators such as silica microtoroids is proposed requiring only one external pump field.

#### ACKNOWLEDGMENTS

The authors thank N. Grosse for contributions to numerical simulations. This research was funded by the Australian Research Council Discovery Project No. DP0987146, the MacDiarmid Institute, and New Zealand Foundation for Research Science and Technology Contract No. NERF-C08X0702.

- 
- [1] E. Schrödinger, Proc. Cambridge Philos. Soc. **31**, 555 (1935).  
 [2] M. A. Nielsen and I. L. Chuang, *Quantum Computation and Quantum Information* (Cambridge University Press, Cambridge, England, 2000).  
 [3] A. Aspect *et al.*, Phys. Rev. Lett. **47**, 460 (1981); D. Salart *et al.*, Nature (London) **454**, 861 (2008).  
 [4] M. F. Yanik and S. Fan, Phys. Rev. Lett. **92**, 083901 (2004).  
 [5] K. Totsuka *et al.*, Phys. Rev. Lett. **98**, 213904 (2007); M. F. Yanik *et al.*, *ibid.* **93**, 233903 (2004).  
 [6] M. Bache *et al.*, Phys. Rev. A **67**, 043802 (2003); M. J. Mallon *et al.*, J. Phys. B **41**, 015501 (2008).  
 [7] A. Kuzmich *et al.*, Nature (London) **423**, 731 (2003); K. S. Choi *et al.*, *ibid.* **452**, 67 (2008); A. M. Marino *et al.*, *ibid.* **457**, 859 (2009).  
 [8] L.-M. Duan *et al.*, Nature (London) **414**, 413 (2001); C. W. Chou *et al.*, Phys. Rev. Lett. **92**, 213601 (2004).  
 [9] A. Furusawa *et al.*, Science **282**, 706 (1998); W. P. Bowen *et al.*, Phys. Rev. A **67**, 032302 (2003).  
 [10] D. K. Armani *et al.*, Nature (London) **421**, 925 (2003); D. S. Weiss *et al.*, Opt. Lett. **20**, 1835 (1995).  
 [11] I. S. Grudinin *et al.*, Opt. Commun. **265**, 33 (2006).  
 [12] M. D. Reid *et al.*, Rev. Mod. Phys. (to be published).  
 [13] T. J. Kippenberg *et al.*, Science **321**, 1172 (2008).  
 [14] D. Elser *et al.*, Phys. Rev. Lett. **97**, 133901 (2006); J. F. Corneey *et al.*, *ibid.* **97**, 023606 (2006).  
 [15] C. W. Gardiner and P. Zoller, *Quantum Noise*, 2nd ed. (Springer-Verlag, Berlin, 2000).  
 [16] L. M. Duan *et al.*, Phys. Rev. Lett. **84**, 2722 (2000).  
 [17] N. B. Grosse *et al.*, Phys. Rev. Lett. **96**, 063601 (2006).  
 [18] W. P. Bowen *et al.*, Phys. Rev. Lett. **90**, 043601 (2003).